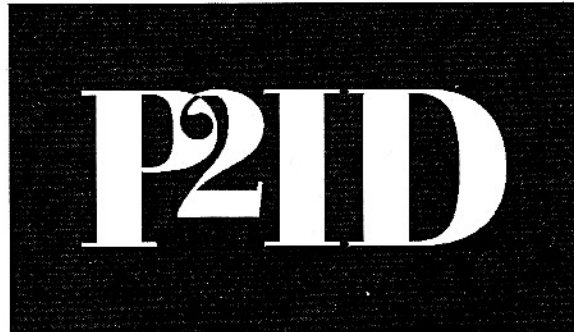

2003 8th International Symposium
on
Plasma- and Process-Induced Damage



**International Symposium on
Plasma- & Process-Induced Damage**

April 24-25, 2003
Altis Semiconductor
Corbeil-Essonnes, France

Technical Co-Sponsors
IEEE/Electron Devices Society
Japanese Society of Applied Physics

ION ORBITS IN ELECTRON SHADING DAMAGE

Tsitsi Madziwa-Nussinov, Donald Arnush, and Francis F. Chen

Electrical Engineering Department, University of California, Los Angeles
Los Angeles, California 90095-1594, USA

In Hashimoto's¹ hypothetical mechanism for electron shading damage, the photoresist at the tops of trenches and vias collects a negative charge from the thermal electrons, creating an electric field (E-field) which prevents electrons from reaching the trench bottom, where a "collector" is located. The ions, accelerated by the sheath electric field, are driven straight into the trench and impinge on the collector, charging it positive if it is isolated. The electric fields inside the trench can also deflect the ions into the sidewalls, causing notching and other deformations of the etch profile². Though this mechanism is widely accepted, it has never been verified in direct experiment. The present effort is to test the hypothesis by scaling the submicron features to macroscopic size so that the currents and potentials inside the trench can be measured and compared with computations. This paper concerns the theoretical part of this work; namely, self-consistent computations of the E-fields and ion orbits inside the trenches.

Such a scaled experiment is possible because of the scale invariance of the governing equations. Let capped (\hat{x}) quantities be dimensional and normal letters be dimensionless. Poisson's equation is

$$\epsilon_0 \hat{\nabla}^2 \hat{V} = e(\hat{n}_e - \hat{n}_i). \quad (1)$$

With the usual definitions $\eta \equiv eV/KT_e$, $\lambda_D^2 \equiv \epsilon_0 KT_e / n_e e^2$, $c_s^2 \equiv KT_e/M$, Eq. (1) can be written

$$\frac{\epsilon_0 KT_e}{n_e e^2} \hat{\nabla}^2 \eta = \lambda_D^2 \hat{\nabla}^2 \eta = 1 - (n_i/n_e). \quad (2)$$

Let s be the scale length of the gradient ∇ , and define $\mathbf{r} \equiv \hat{\mathbf{r}}/s$, so that $\nabla^2 = s^2 \hat{\nabla}^2$, yielding

$$\nabla^2 \eta = \frac{s^2}{\lambda_D^2} \left(1 - \frac{n_i}{n_e} \right) \approx 0. \quad (3)$$

In microtrenches, $s \ll \lambda_D$; the r.h.s. can be neglected, and we need only solve Laplace's equation $\nabla^2 \eta = 0$ subject to the boundary conditions $\eta = \eta_b(\mathbf{r}_b)$ at $\mathbf{r} = \mathbf{r}_b$. The solution would be the same as that of the dimensional problem $\hat{\nabla}^2 \eta = 0$ with the boundary conditions $\eta = \eta_b(\hat{\mathbf{r}}_b)$ at $\hat{\mathbf{r}} = \hat{\mathbf{r}}_b$. Thus, only the aspect ratio of the trench matters and not its absolute size, as long as the Debye length λ_D is $\gg s$. In other words, the space charge deep inside the sheath is negligible. The problem in the scaled experiment is to create a plasma with sufficiently large λ_D ; this will be presented in another paper.

The ion trajectories are computed from

$$\frac{d^2 \hat{\mathbf{r}}}{dt^2} = -\frac{e}{M} \hat{\nabla} V = -\frac{e}{M} \frac{KT_e}{e} \nabla \eta = -c_s^2 \hat{\nabla} \eta. \quad (4)$$

In terms of \mathbf{r} , this becomes $s^2 d^2 \mathbf{r} / dt^2 = -c_s^2 \nabla \eta$; and defining $\tau \equiv c_s t / s$, we have

$$d^2 \mathbf{r} / d\tau^2 = -\nabla \eta, \quad (5)$$

which has the same form as Eq. (4), regardless of s . Thus, the ion orbits are geometrically the same on any scale; only the time scale is changed. The computations are in these scale-independent dimensionless units. Collisions are completely negligible.

The computational grid is shown in Fig. 1. A block of dielectric with $\epsilon \approx 4$ is surrounded by a vacuum sheath region bounded by a conductor representing the sheath edge, S dimensionless units away. In practice S is much larger than the feature size and its value is not significant. The bottom of the dielectric block is the substrate being etched, and the trench

grows in the direction of increasing y . The bottom surface would normally be photoresist and is divided into cells x_j , while the trench walls are divided into smaller cells y_j . The dielectric has width $2L = 14$ and height $H = 10$, while the trench has width $2W$ and depth D , with aspect ratio $A_R = 2W/D$. Ions are injected vertically from the $V = V_s$ surface at $y = 0$ with the Bohm velocity c_s . The “bottom” of the trench (at the top) is covered with a collector at potential V_c .

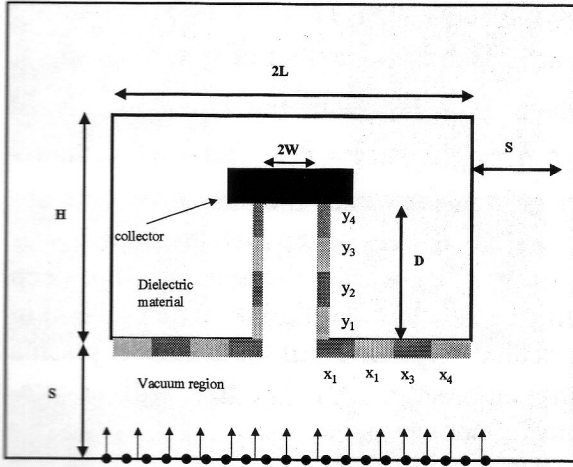


Fig. 1

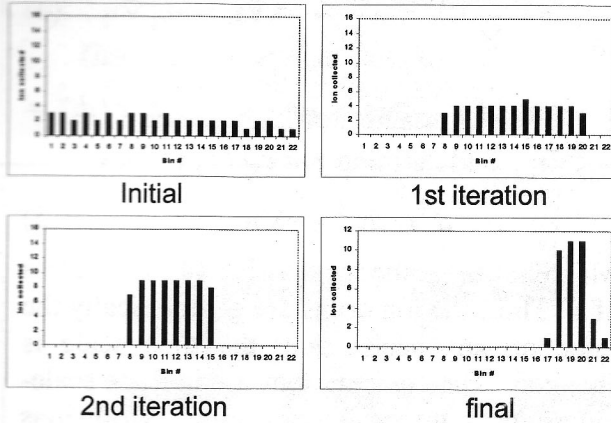


Fig. 2: $A_R = 7$, $V_c = -18V$

The electrons are assumed to be Maxwellian and follow the Boltzmann relation

$$n_e/n_s = \exp[(V - V_s)/T_{eV}], \quad (6)$$

where $T_{eV} \equiv KT_e/e$,

and $n_e = n_i = n_s$ at the sheath edge.. As long as $V_c < 0$, electrons are in a repelling potential everywhere, and this relation holds in any

geometry. The potential on a floating surface is found by equating the electron and ion fluxes. The electron flux is

$$\Gamma_e = n_e v_r = n_s \exp[(V - V_s)/T_{eV}] v_r, \quad (7)$$

where $v_r = (KT_e/2\pi m)^{1/2}$ is the random thermal velocity normal to a surface. The ion flux at $y = 0$ is simply

$$\Gamma_0 \equiv \Gamma_i(0) = n_s c_s = n_s (KT_e/M)^{1/2}. \quad (8)$$

In the absence of a trench, the substrate surface at $y = 6$ charges to the usual floating potential given by $\Gamma_i(6) = \Gamma_i(0) = \Gamma_e$:

$$(V_f - V_s)/T_{eV} = -\ln(M/2\pi m)^{1/2} \approx -4.68 \quad (9)$$

for argon. We now set $V_s = 0$, so that the computation is in a grounded box. Since V_s is $\approx -1/2 T_{eV}$ relative to the plasma, V_f is about $-5.18 T_{eV}$ relative to the plasma or $\approx -15V$ for $KT_e = 3$ eV in argon.

In the computation, let N be the number of ions ($\approx 10^4$) emitted at $y = 0$ over a surface area LZ per unit time, where Z is a length in the z direction. The emitted ion flux is $\Gamma_0 = N/LZ = n_s c_s$. If N_j ions strike a surface cell of width Δx_j , the ion flux to that cell is $\Gamma_{ij} = N_j / \Delta x_j Z$. The ratio of this to the undisturbed flux Γ_0 is then

$$R(x_j) = (N_j/N)(L/\Delta x_j) = F(x_j)(L/\Delta x_j)$$

where $F(x_j)$ is the fraction of all ions that end up in cell x_j . Fluxes $\Gamma(y_j)$ to the trench wall are normalized similarly. The electron flux Γ_{ej} to a cell is $n_s v_r \exp(V_j/T_{eV})$. Equating this to the ion flux $\Gamma_{ij} = n_s c_s R(x_j)$ and using Eq. (9), we find for floating potential of that cell

$$V(x_j) = T_{eV} [\ln(F_j L/\Delta x_j) - 4.68] \quad (11)$$

relative to the sheath edge.

Ion orbits are computed first with all the insulating surfaces at V_f and the collector at V_c . N_j is then found, and the potential distribution $V(x_j)$ is calculated and used in the first iteration. The ion orbits are then recalculated, giving data for the next iteration. This is continued until N_j and $V(x_j)$ converge to steady

values. When no ion falls on a cell, Eq. (11) diverges. In that case, we assume that the cell actually receives one ion or a fraction of an ion, resulting in $V(x_j) \approx -40V$. The results are not sensitive to this approximation, since V varies logarithmically with n_i . Figure 2 shows the distribution of ions N_j to the cells y_j on the trench wall after several iterations; the entrance is on the left, and the collector on the right. In some cases, $V(x_j)$ does not converge but oscillates between two or three patterns after 25 iterations. This is caused by the fact that ions are kinematically shielded from some cells, and the location of these cells depends on the fields from the previous iteration. In these cases, the patterns are so similar that an average pattern can be used.

Thus, the ions receive a kick as they enter and then coast to the collector. Since the E-fields are affected by the shape of the corner, we have rounded it into an arc, as shown in Fig. 4.

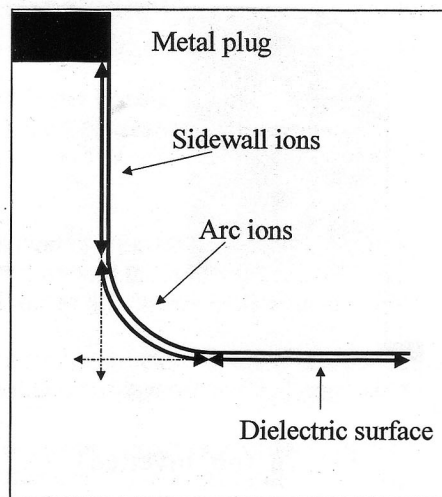


Fig. 4

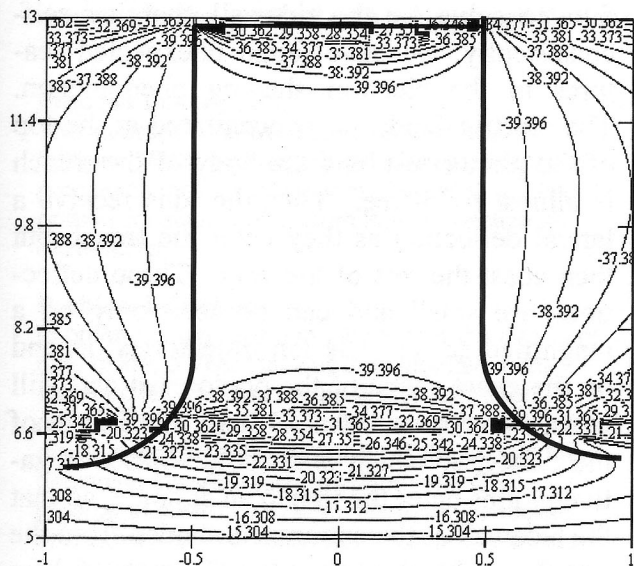


Fig. 3

Figure 3 shows equipotential lines for $V_c = -40V$ and $A_R = 7$ (not to scale). It is seen that the E-fields are concentrated near the trench entrance, and the interior is almost field-free.

This has a large effect on the ion distribution on the sidewall, as seen in Fig. 5. To test this further, we added small bumps to the arc section, and these affect the ion orbits also. Thus, as the photoresist shape changes during an etch, the ion orbits change. Figure 6 shows the ion distribution as V_c is varied at $A_R = 3$ and as A_R is varied at $V_c = -18V$. In general, there are so few ions hitting the sidewall that they cannot cause changes in the etch profile.

The situation is clear in the sample orbits shown in Fig. 7. On a real scale, the ion trajectories are almost straight; very few hit the sidewalls. When the y-axis is shrunk by a factor 20 (Fig. 7b), it is seen that the field of the collector affects the ions before they enter the trench. The sidewall cells at the entrance are shielded from the ion flux—an ion-shielding effect.

V_c	Corner	N	To sidewall	To collector
-18V	Square	10593	21 (0.2%)	830 (7.8%)
-18V	Curved	10606	31 (0.3%)	1201 (11%)
-26V	Square	10593	34 (0.3%)	813 (7.7%)
-26V	Curved	10606	0 (0.0%)	1201 (11%)

Fig. 5

V_c	S.W.	Coll.	A_R	S.W.	Coll.
-18	65	778	3	65	778
-22	57	785	5	34	1005
-26	44	822	7	17	1184
-40	32	834			
-60	0	866			

Fig. 6

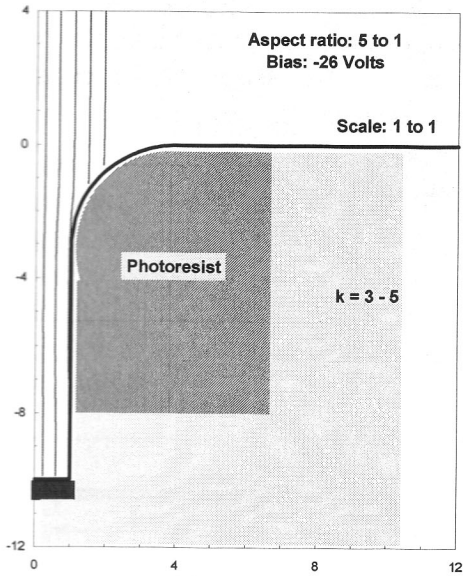


Fig. 7a (not inverted)

We have also examined cases where part of the sidewall is conducting or the collector is large (Fig. 8a) and also when there are neighboring trenches (Fig. 8b). The general result is that the field lines are straighter and there are fewer sidewall ions when the collector or AR is large.

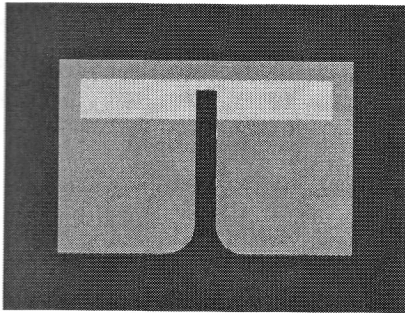


Fig. 8a

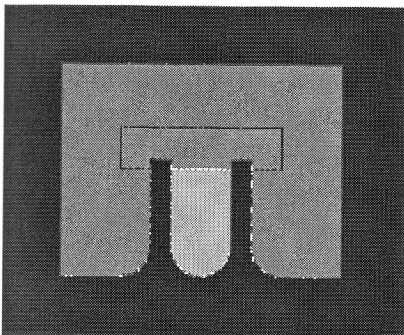


Fig. 8b

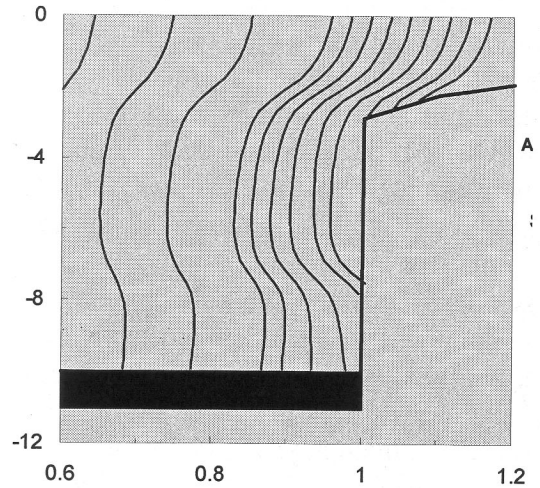


Fig. 7b

In summary, by using an iterative procedure to solve for the sidewall charging self-consistently, we have found unexpected features in the electron shading phenomenon. The electric fields are concentrated at the top of the photoresist, and the body of the trench is almost field-free. Thus the ions receive a lateral deflection as they enter the trench but then coast the rest of the way. These deflections are small and can be seen only on a magnified scale. The ion trajectories depend on the exact shape of the photoresist and will change during an etch. Due to the E-field of the collector, which is substrate-biased negatively, ions enter the trench at an angle, so that the sidewall at the entrance is shaded from the ion flux. In any case, the fraction of ions striking the sidewall is too small to affect the etch profile. This is also true for etching into a conductor. An asymmetric collector can move ions to one side, as with neighboring trenches. A deep trench, surprisingly, has fewer sidewall ions. This is because the field lines are more vertical at the entrance. This paper is only an abstract of numerous computational results which will eventually be presented in a full paper.

¹ K. Hashimoto, *Jpn. J. Appl. Phys.* **33**, 6013 (1994).

² G.S. Hwang and K.P. Giapis, *J. Vac. Soc. Technol. B* **15**, 70 (1997).